25th ABCM International Congress of Mechanical Engineering
October 20-25, 2019, Uberlândia, MG, Brazil

COB-2019-1084
Vehicle stability Control Based On Linear Quadratic Regulator

Zoé Roberto Magalhães Júnior
André Murilo de Almeida Pinto
Renato Vilela Lopes
Universidade de Brasília, Faculdade do Gama, St. Leste Projeção A - Gama Leste, Brasília - DF, 72444-240
zr.magal@gmail.com,andremurilo@unb.br,rvlopes@unb.br

Abstract.*In this work, an Electronic Stability Control (ESC) is proposed for the correction of undesired movements, which deviate the vehicle from the driver-controlled trajectory and threatens the driver to lose control of the steering. A Linear Quadratic Regulator is employed to compute the correction torques transferred to wheels. The LQR is defined based on a linear model that includes side-slipping, yawing and rolling motions, such that, besides keeping the vehicle in the desired trajectory by correcting of yaw-rate and side-slip, the LQR is able to take into account the actuation effect on rolling motion. Model-in-the-loop simulations are performed, where the proposed algorithm is tested on control of the vehicle presented by a nonlinear model that includes the body's longitudinal, lateral, yawing and rolling movements and the rotation of four wheels. Those simulations also include a driver model to generate the steering wheel angle. Results from simulation for double lane change maneuver show that the proposed system is effective to keep the steering stable during maneuvers that can not be performed without ESC assistance.*

Keywords: *ESC , LQR and DYC*

1. INTRODUCTION

Vehicle Stability Controllers (VCS) are active assistance systems that help the driver to keep the vehicle on the driven path and avoid conditions in which driving is too difficult. Lateral stability of the vehicle can be improved by controlling the yaw rate, which keeps the vehicle with correct orientation to perform the desired maneuver and correcting the side-slip, which prevents the vehicle from slipping sideways off the desired path.

A successful strategy of actuation is the Direct Yaw-moment Control (DYC), in which the rotational torque of wheels is controlled to manipulate the forces generated by tires to achieve the required yaw moment. One benefit of DYC is the fact that at high side slipping the movement remains responsive to the rotation speed of wheels (LIAN *et al.*, 2015; Mousavinejad *et al.*, 2015; Guo *et al.*, 2017).

In respect with the control technique, researches have been performed in the past years to explore in ESC design the benefits of advanced control techniques, made possible by the increased computational power available for embedded systems, such as Model-based Predictive Control (MPC) (Guo *et al.*, 2017; Jalali *et al.*, 2017; Nahidi *et al.*, 2017),Sliding Mode Control (SMC) (Rajamani and Piyabongkarn, 2013; Le and Chen, 2015; Liu *et al.*, 2017),backstepping technique (Zhou and Liu, 2010) and robust gain schedule (Jin *et al.*, 2015, 2017). But applications of classical control such that Linear Quadratic Regulator (LQR), which is an optimal controller that does not require much computational power, has not been considered in the same way.

As important as the definition of control architecture is the choosing of the quality assurance methodologies used in ESC design. Model-in-the-loop (MIL) is a useful methodology that contributes to reducing the number of test runs and damage risk at the during the final validation stages of experimental tests. Experimental tests of ESC embedded in a real car require a controlled environment, which makes each test run expensive, and at this stage a fault detection impacts on engineering cost with redesign and production.

In MIL, computational simulations are performed to test the ESC algorithm on control of a vehicle represented by a simulation model. These simulations can be performed before the implementation of hardware and firmware of the embedded control system. In addition to early fault detection, MIL enables the observation of variables that are difficult to be physically measured, and simulation of maneuvers that are hard to be reproduced in experimental tests (Plummer, 2006; Ciceo *et al.*, 2015).

Designs of LQR-based ESC has been presented in the literature. In (Zheng *et al.*, 2006), an LQR-based ESC is designed to compute the additional yaw moment required to improve lateral stability. The model used In (Zheng *et al.*, 2006) for LQR design includes side-slip and yaw motion, without consideration of rolling effects. In (Mashadi *et al.*, 2011), another LQR-based ESC is present, where the control signals are the difference between left and right clutch torques and the correcting yaw moment from breaking. The LQR is defined in (Mashadi *et al.*, 2011) based on a linear

model that includes rolling motions. An LQR-based ESC design also is presented in (Yogurtcu *et al.*, 2015) to control the traction/breaking generated by electric motors on the rear axis. In (Yogurtcu *et al.*, 2015), a linear model with roll degree-of-freedom is used for the definition of the gain matrix. Within the simulation models presented in those works to evaluated proposed LQR-based ESC, only in (Mashadi *et al.*, 2011) a model is included to simulate the driver behavior on steering wheel command.

In this work, an LQR-based ESC is designed and MIL simulations are performed to evaluate its effectiveness.

The contributions of this work are:

- Development of an LQR-based ESC that gives the traction/braking torque transferred to each wheel taking into account the influences of roll motion on lateral stability and the influences of actuation on roll motion.
- Presentation of MIL simulation environment for evaluation of ESC systems which control inputs are the torque transferred to the wheels, which includes, in addition to simulation of vehicle movement, a model for simulation of driver behavior on steering wheel command
- Evaluation of proposed ESC with proposed MIL testing in the following scenarios:
  - ESC assistance is not required
  - ESC assistance is required and vehicle response is close to the predicted by the linear model used for control design
  - ESC assistance is required and the vehicle speed is higher than the constant assumed in the linear model used for control design
  - ESC assistance is required, and vehicle response is different from the predicted by the linear model used for control design, due to disturbances in parameters of the vehicle model.

In proposed ESC design, the LQR gain is defined based on a vehicle linear model more representative then the 2DOF bicycle model, by including the rolling motion, assuming longitudinal speed constant and enabling additional rolling control. The roll motion has a strong influence on vehicle movement because it directly affects lateral and yaw motions and changes the forces generated by tires, by changing steer and camber angle and provoking the vertical load transfer between tires.

2. Vehicle Dynamic

A vehicle model is needed for the implementation of the MIL environment and obtaining the linear model used for control design. The reference model adopted in this work considers lateral, yaw and roll motions The Fig. 1 shows this model represented by the following equations of motions (Li *et al.*, 2017; Dahmani *et al.*, 2016; Mashadi *et al.*, 2010; Zheng *et al.*, 2006):

Longitudinal motion

$$\begin{aligned} m\left(\dot{u}-\dot{\psi}v\right)-m_s h_s\dot{\psi}\dot{\phi} =& -\sin(\delta_f)(F_{yfl}+F_{yfr})+\cos(\delta_f)(F_{xfl}+F_{xfr}) \\ & -\sin(\delta_r)(F_{yrl}+F_{yrr})+\cos(\delta_r)(F_{xrl}+F_{xrr}) \end{aligned} \tag{1}$$

Lateral motion

$$\begin{aligned} m\left(\dot{v}-\dot{\psi}u\right)-m_s h_s\ddot{\phi} =& \cos(\delta_f)(F_{yfl}+F_{yfr})+\sin(\delta_f)(F_{xfl}+F_{xfr}) \\ & +\cos(\delta_r)(F_{yrl}+F_{yrr})+\sin(\delta_r)(F_{xrl}+F_{xrr}) \end{aligned} \tag{2}$$

Yaw motion

$$\begin{aligned} I_{zz}\ddot{\psi}-I_{xz}\ddot{\phi} =& a(\cos(\delta_f)(F_{yfl}+F_{yfr})+\sin(\delta_f)(F_{xfl}+F_{xfr})) \\ & -b(\cos(\delta_r)(F_{yrl}+F_{yrr})+\sin(\delta_r)(F_{xrl}+F_{xrr})) \\ & +\frac{t_f}{2}(\cos(\delta_f)(F_{xfr}-F_{xfl})-\sin(\delta_f)(F_{yfr}-F_{yfl})) \\ & +\frac{t_r}{2}(\cos(\delta_r)(F_{xrr}-F_{xrl})-\sin(\delta_r)(F_{yrr}-F_{yrl})) \end{aligned} \tag{3}$$

Roll motion

$$I_{xx}\ddot{\phi}-I_{xz}\ddot{\psi} = m_s h_s\left(\dot{v}+\dot{\psi}u\right)+m_s h_s g\sin(\phi)-\left(k_{\phi f}+k_{\phi r}\right)\phi-\left(c_{\phi f}+c_{\phi r}\right)\dot{\phi} \tag{4}$$

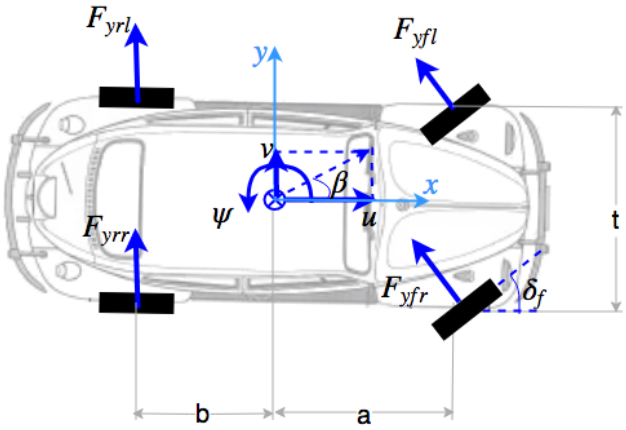

Figure 1. Vehicle dynamic model

where v denotes the lateral speed, u the longitudinal speed, ϕ the roll angle, ψ the yaw angle, δ_f and δ_r front and rear steering angle, m the vehicle total mass, m_s the suspense mass above rolling axes, h_s the height of rolling axes, I_{xx} and I_{zz} the yawing and rolling inertial moments, respectively, I_{xz} the inertial product related to yawing and rolling, $k_{\phi i}$ the rolling stiffness coefficient, c_ϕ the rolling damping coefficient, M_u a external yaw moment, and F_{yfl},F_{yfr},F_{yrl},F_{yrr} are lateral tire forces.

The Magic Formula (MF) of Pacejka is an empirical formulation derived from experimental tests that can be used to compute forces acting on tires, as shown in (Pacejka, 2006). In the general formulation of MF , the forces acting on an tire is obtained as follows:

$$F(x) = D\sin(Sv_i C\arctan(B(1-E)(x+Sh_i) + E\arctan(B(x+Sh_i)))) \tag{5}$$

in which, for computation of the lateral force F_{yi} of ith, the argument x is the tire side-slip angle α_i and B, C, D, E, Sh_i, Sv_i are defined by MF coefficients a_n, $\quad n = 0, 1 \ldots 14$ and the camber angle γ_i as follows:

$$\begin{aligned}
&C = a_0 && D = F_{zi}(a_1 F_{zi} + a_2) \\
&B = \frac{a_3 \sin(2\arctan\frac{F_{zi}}{a_4})}{CD}(1 - a_5|\gamma_i|) && E = a_6 F_{zi} + a_7 \\
&Sh_i = a_8\gamma_i + a_9 F_{zi} + a_{10} && Sv_i = \left(a_{11}F_{zi}^2 + a_{12}F_{zi}\right)\gamma_i + a_{13}F_{zi} + a_{14} \\
&i = fl, fr, rl, rr
\end{aligned} \tag{6}$$

for computation of longitudinal force F_{xi} of ith wheel, the argument x is the tire slip ratio λ_i and B, C, D, E, Sh_i, Sv_i are defined by MF coefficients b_n, $\quad n = 0, 1 \ldots 14$ as follows:

$$\begin{aligned}
&C = a_0 && D = F_{zi}(b_1 F_{zi} + b_2) \\
&B = \frac{b_3 \sin(2\arctan\frac{F_{zi}}{b_4})\exp(b_5 F_{zi})}{CD} && E = b_6 F_{zi}^2 + b_7 F_{zi} + b_8 \\
&Sh_i = b_9 F_{zi} + b_{10} && Sv_i = 0 \\
&i = fl, fr, rl, rr
\end{aligned} \tag{7}$$

F_{zi} denotes the vertical load in ith wheel given by (Li *et al.*, 2017; Zheng *et al.*, 2006):

$$\begin{aligned}
F_{zfl} &= \frac{mgb}{2l} - \frac{ma_x h}{2l} - \frac{ma_y ah}{lt_f} - \frac{k_{\phi f}\phi}{t_f} - \frac{c_{\phi f}\dot{\phi}}{t_f} & F_{zfr} &= \frac{mgb}{2l} - \frac{ma_x h}{2l} + \frac{ma_y ah}{lt_f} + \frac{k_{\phi f}\phi}{t_f} + \frac{c_{\phi f}\dot{\phi}}{t_f} \\
F_{zrl} &= \frac{mga}{2l} + \frac{ma_x h}{2l} - \frac{ma_y ah}{lt_r} - \frac{k_{\phi r}\phi}{t_r} - \frac{c_{\phi r}\dot{\phi}}{t_r} & F_{zrr} &= \frac{mga}{2l} + \frac{ma_x h}{2l} + \frac{ma_y ah}{lt_r} + \frac{k_{\phi r}\phi}{t_r} + \frac{c_{\phi r}\dot{\phi}}{t_r}
\end{aligned} \tag{8}$$

where a and b are the distances from the center of gravity to the front and rear axis, h the height of the center of gravity, t_f and t_r the front and rear track width, l the wheelbase, $c_{\phi f}$ and $c_{\phi r}$ the front and rear roll damping coefficient, $k_{\phi f}$ and $k_{\phi r}$ the front and rear roll stiffness.

The side-slip angle of each wheel is given by:

$$\begin{aligned} \alpha_{fl} &= \delta_f - \arctan\left(\frac{v + a\dot{\psi}}{u - \frac{t_f}{2}\dot{\psi}}\right) \quad \alpha_{fr} = \delta_f - \arctan\left(\frac{v + a\dot{\psi}}{u + \frac{t_f}{2}\dot{\psi}}\right) \\ \alpha_{rl} &= -\arctan\left(\frac{v - b\dot{\psi}}{u - \frac{t_r}{2}\dot{\psi}}\right) \qquad \alpha_{rr} = -\arctan\left(\frac{v - b\dot{\psi}}{u + \frac{t_r}{2}\dot{\psi}}\right) \end{aligned} \tag{9}$$

In order to consider the effects of roll motion on tire dynamic, the camber angle of four wheels are considered in this work ideally the same, simplified as follows:

$$\gamma = K_\gamma \phi \tag{10}$$

K_γ denotes the camber-by-roll gradient, which represents variation of camber due to rolling given by $K_\gamma = \frac{\partial \gamma}{\partial \phi}$ (D. Gillespie, 2000).

The slip ratio λ_i of is the ratio between the vehicle longitudinal speed and the ideal speed given by total conversion of wheel rotation in longitudinal speed, defined as:

$$\lambda_i = \frac{R_{eff}\omega_i - u}{max(R_{eff}\omega_i, u)} \tag{11}$$

where R_{eff} is the effective radius of the tire and ω_i is the angular speed, obtained from the equation of rotational motion of each transmission shaft is:

$$\dot{\omega_i} = \frac{T_i - R_{eff}F_{xi}}{J_w} \tag{12}$$

where T_i is the torque transferred to the ith wheel and J_w is the moment of inertia of the transmission shaft.

And the steering angle of wheels is considered as composed by a part relating to the driver's command and a part generated by rolling motion, which, for a passenger car that only front wheels are controlled by the steering wheel, the passenger car of each wheel is given by:

$$\delta_{fl} = \frac{\delta_D}{I_s} + \frac{\partial \delta_{fl}}{\partial \phi}\phi \qquad \delta_{rl} = \frac{\partial \delta_{rl}}{\partial \phi}\phi \qquad \delta_{fr} = \frac{\delta_D}{I_s} + \frac{\partial \delta_{fr}}{\partial \phi}\phi \qquad \delta_{rr} = \frac{\partial \delta_{rr}}{\partial \phi}\phi \tag{13}$$

where δ_D is the steering wheel angle, I_s is the steering ratio coefficient, and $\partial\delta_i/\partial\phi$ is the steer-by-roll coefficient of ith wheel.

The Equations from 1 to 14 represents the reference model of vehicle dynamic adopted in this study. Ideally, a vehicle should move without side slipping, with total speed vector parallel to vehicle longitudinal axis. Therefore, the metric used to analyze the lateral0 performance is the angle between the actual speed vector and the vehicle longitudinal axis, known as side-slip angle β given by:

$$\beta = \arctan v/u \tag{14}$$

2.1 Linear model

A linear model of vehicle movement is needed for definition of LQR gain matrix. This model is obtained from linearization of the model presented in previous section, for small roll and side-slip angles, such that $\sin(\phi) \approx \phi$ and $\beta \approx v/u$. The resultant model is expressed by the following equations:

Lateral motion:

$$mu\left(\dot{\beta} + \dot{\psi}\right) - m_s h_s \ddot{\phi} = \sum F_y \tag{15}$$

Yaw motion:

$$I_{zz}\ddot{\psi} - I_{xz}\ddot{\phi} = a(F_{yfl} + F_{yfr}) - b(F_{yrl} + F_{yrr}) + \frac{t_f}{2}(F_{xfr} - F_{xfl}) + \frac{t_r}{2}(F_{xrr} - F_{xrl}) \tag{16}$$

Roll motion:

$$I_{xx}\ddot{\phi} - I_{xz}\ddot{\psi} = m_s h_s u(\dot{\beta} + \dot{\psi}) + m_s h_s g\phi - (k_{\phi f} + k_{\phi r})\phi - (c_{\phi f} + c_{\phi r})\dot{\phi} \tag{17}$$

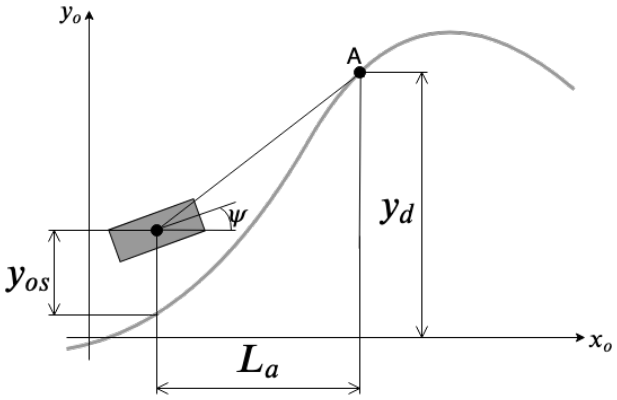

Figure 2. Illustration of driver modelling.

For smalls tire slip and camber angles, the lateral force generated by tires is approximated by:

$$F_{yi} = C_{\alpha i}\alpha_i + C_{\gamma i}\gamma \tag{18}$$

$C_{\alpha i}$ and $C_{\gamma i}$ denote cornering stiffness and camber stiffness coefficients, which can be obtained from Equations 5 and 18 (Pacejka, 2006) as follows:

$$C_{\alpha i} = \left.\frac{\partial F_{yi}}{\partial \alpha_i}\right|_{a_x,a_y,\gamma,\alpha,\phi,\dot{\phi}=0} \qquad C_{\gamma i} = \left.\frac{\partial F_{yi}}{\partial \gamma_i}\right|_{a_x,a_y,\gamma,\alpha,\phi,\dot{\phi}=0} \tag{19}$$

The front and rear wheels slip angle are approximated by linear functions of vehicle slip angle β, yaw rate $\dot{\psi}$ and front wheels steer angle δ_f (Zheng and Shyrokau, 2019; Zheng *et al.*, 2006):

$$\alpha_f = -\beta - \frac{a\dot{\psi}}{u} + \delta_f \qquad \alpha_r = -\beta + \frac{b\dot{\psi}}{u} \tag{20}$$

Neglecting the variation of angular speed of wheels, e.g. as in Shoutao Li, Di Zhao, Luyu Zhang and College (2017), the longitudinal force acting on the tire can be approximated by:

$$F_{xi} = T_i/R_{eff} \tag{21}$$

The torque that can be transferred for each wheel is constrained by limitations of the actuation system. In this study, the absolute value of the torques transferred to wheels is assumed as constrained at value denoted by T_{th}.

From Equations 15-21 is possible to obtain the linear model in the continuous time state space representation:

$$\begin{aligned} &\dot{x} = A \cdot x + B \cdot u + B_d \cdot u_d \\ &x = \begin{bmatrix}\beta & \dot{\psi} & \dot{\phi} & \phi & \omega_{fl} & \omega_{fr} & \omega_{rl} & \omega_{rr}\end{bmatrix}^T \qquad u = \begin{bmatrix}T_{fl} & T_{fr} & T_{rl} & T_{rr}\end{bmatrix}^T \qquad u_d = \delta_f \end{aligned} \tag{22}$$

in which x denotes the state vector, u the control input, u_d is the known disturbance vector (input of the plant that is not controlled by ESC) δ_f the disturbance and $A \in R^{8\times 8}$ and $B \in R^{8\times 4}$ are the state and input matrices of state-space representation, respectively, and B_d is the disturbance input matrix.

3. Intelligent Driver Model

In addition to the vehicle model, the MIL environment developed in this work also considers an intelligent driver model. The model presented in (Reński, 2001) is used to generate the steering wheel angle δ_D, by simulating the driver reaction to vehicle movement with respect to the desired path. The Fig. 3 illustrates this model, which considers that the simulated driver acts to fix the movement direction, aiming to achieve the speed direction for moving towards a target point A at a distance L_a, based on observation of current position y_{os}, desired position y_d and yaw angle ψ. Fig. 2 shows the block diagram of this control law. The parameters of this model are the distance L_a from the vehicle position to target point, actuation delay T_k and a steering gain coefficient W that represents driver expertise.

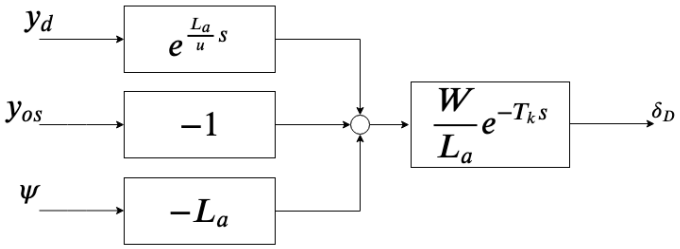

Figure 3. Block diagram of driver model.

4. Control System

The proposed control algorithm gives as control input the traction/braking torque transferred to each wheel for correction of errors in yaw rate, side-slip angle, and roll motions.

A maneuver performed with a minimum roll angle is desired for the reduction of rollover risk and increasing passenger comfort. And a maneuver with a minimum lateral slip angle is desired for avoiding the driver from losing vehicle control and the vehicle from sliding sideways off the safe path. As the equations of motion suggest, some maneuvers can not be performed without rolling or null side slipping. However, to spare the computational time for dynamically computing the minimum values, the desired values are assumed equal to zero. The safe-desired yaw rate depends on the driver intention, represented by the front wheels steering angle, and vehicle speed, its value can be computed as follows (Zheng *et al.*, 2006):

$$\dot{\psi}_d = \begin{cases} \frac{u\delta_f}{l+lK_u u^2}, & \text{if} |\dot{\psi}_d| \leq \left|\frac{\mu g}{u}\right| \\ sign(\delta_f)\left|\frac{\mu g}{u}\right|, & \text{otherwise} \end{cases} \qquad K_u = \frac{m}{l^2}\left(\frac{b}{C_{\alpha r}} - \frac{a}{C_{\alpha f}}\right) \tag{23}$$

where $C_{\alpha r}$ and $C_{\alpha f}$ are rear and front cornering stiffness due to tire slip angle, respectively.

Figure 4 presents the system block diagram. The next control sample $u[k+1]$ is update once every sampling time with the control law $u[k+1] = K\tilde{x}[k]$, in which $\tilde{x}[k]$ is the current sample of states error.

Therefore, the discrete LQR for the continuous plant is used to define the gain matrix K that minimizes the cost function $J = \int_0^\infty \tilde{x}^T Q\tilde{x} + u^T R u dt$, where Q and R are diagonal matrices that weights states errors and command energy, respectively. The Matlab function **lqrd** is useful for finding the K matrix of the discrete LQR for the continuous plant, whose arguments are the sampling time and the linear continuous-time state-space model.

A non-null actuation is performed by LQR when the states are different from their desired values, even when these errors do not mean a risk of lateral instability. In order to avoid this unnecessary actuation, the ESC remains inactive while side-slip angle and yaw error is not greater than thresholds. And to avoid constant switching of ESC activation, the ESC is activated when the condition $\beta_{th} \leq \beta$ or $\psi_{eth} \leq \psi_e$ is fulfilled for a minimum period T_{on}, and it is deactivated when none of those conditions is fulfilled for a minimum period T_{off}.

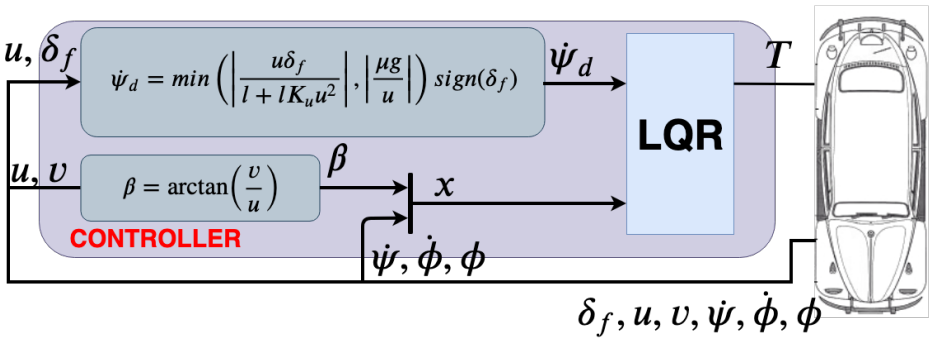

Figure 4. Control system

Table 1. Parameters of simulation models of vehicle and driver

Param.	Value	Param.	Value	Param.	Value	Param.	Value
a	1.1 m	b	1.3 m	t_f	1.4 m	t_r	1.41 m
h_s	0.55 m	h	0.6 m	m	1070 Kg	m_s	900 Kg
I_{zz}	2100 Kgm^2	I_{xx}	500 Kgm^2	I_{xz}	47.0 Kgm^2	I_s	20
$c_{\phi f}$	1050 Nms/rad	$c_{\phi r}$	1050 Nms/rad	$k_{\phi f}$	32795 Nm/rad	$k_{\phi r}$	32795 Nm/rad
$\partial\delta_f/\partial\phi$	0.1	$\partial\delta_r/\partial\phi$	-0.1	L_a	$1.2 \cdot u$	W	0.2
μ	0.75	T_k	0.2				
a_0	1.3	a_1	-49	a_2	1216	a_3	1632
a_4	11	a_5	0.006	a_6	-0.04	a_7	-0.4
a_8	0.003	a_9	-0.002	a_{10}	0		

Table 2. Parameters of control design

Param.	Value	Param.	Value	Param.	Value	Param.	Value
a	1.1 m	b	1.3 m	h_s	0.55 m	m_s	900 Kg
I_{zz}	2100 Kgm^2	I_{xx}	500 Kgm^2	I_{xz}	47.0 Kgm^2	$c_{\phi f}$	1050 Nms/rad
$c_{\phi r}$	1050 Nms/rad	u	100km/h	$k_{\phi f}$	32795 Nm/rad	$k_{\phi r}$	32795 Nm/rad
$\partial\delta_f/\partial\phi$	0.1	$\partial\delta_r/\partial\phi$	-0.1	$C_{\alpha fl}$	45292μ N/rad	$C_{\gamma fl}$	-86340 μ N/rad
$C_{\alpha fr}$	45292μ N/rad	$C_{\gamma fr}$	-86340μ N/rad	$C_{\alpha rl}$	39018μ N/rad	$C_{\gamma rl}$	-61455μ N/rad
$C_{\alpha rr}$	39018μ N/rad	$C_{\gamma rr}$	-61455μ N/rad				
T_{th}	200 Nm	μ	0.75	β_{th}	0.1 rad	T_{on}	0.08 s
ψ_{eth}	0.1 rad/s	T_{off}	0.8s	$diag(Q)$	$(66.0, 248.9, 374.2)$	R	$10^{-5}I^{4\times4}$

5. Results

5.1 Tuning of LQR parameters

The proposed ESC control is designed based on the 3DOF linear model presented in section 4. The parameters Q and R of LQR design were defined with the values that minimize a function that weights the states errors, trajectory error, and control energy, all accumulated from results of simulations for DLC maneuver at 80km/h, 100km/h, and 120km/h. The following equation express the cost function defined:

$$J_C = \int_0^{10} \left(|y_e(t)| + |\psi_e(t)| + 10\,|\beta(t)| \quad +10\,|\phi(t)| + 0.01 u^T(t) u(t) \right) \mathrm{d}t \tag{24}$$

where t denotes the simulation time, y_e the error between desired and vehicle path and ψ_e the yaw rate error.

This optimization problem was solved with the function **particleswarm** provided by Matlab, with **fmincon** method enabled, such that a swarm stochastic search is performed to find the optimum values of Q and R. The Table 2 shows the parameters used for control design.

5.2 Results from MIL simulation

Model-in-the-loop simulations were performed for double lane change (DLC) testing of standard No. ISO 3888:1975 as presented in Reński (2001), in which, boundaries of lateral displacement from the desired path are imposed for approval of the lateral performance. The MIL environment is implemented in this work by combining the vehicle and driver models presented in Section 2and Section 3.Table 1 shows the parameters used in these simulations.

5.2.1 Tire dynamic

Figure 5 shows the relationship between lateral force generated by tires and the tire slip angle obtained from Equation 5 and its linear approximation shown in Equation 18. From this result is possible to observe that Equation 18 is a good approximation for tire slip angle less than 5 degrees. Also is possible to see that, in the considered vehicle, the camber angle considered does not have a significant influence on forces generated by tires.

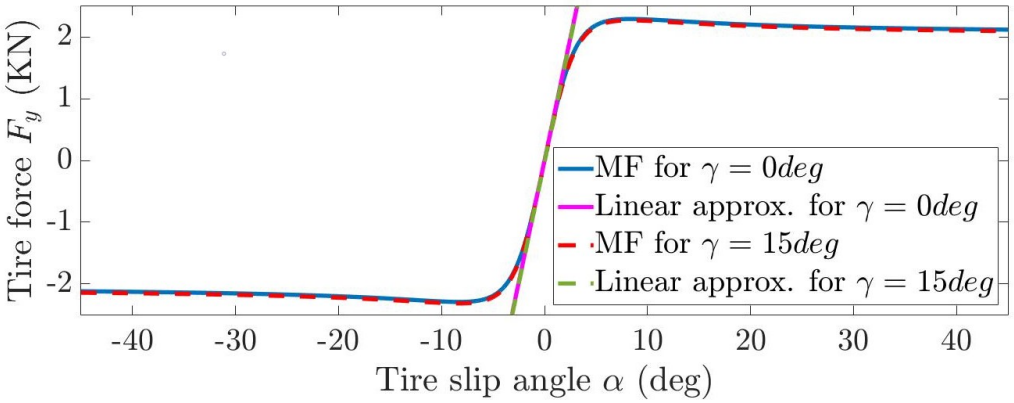

Figure 5. Relationship between tire forces and side slip angle obtained from Pacejka's Magic Formula (Eq. 5) and from linear approximation (Eq. 18) for camber angle equal to zero and 15 degrees, when vertical load is 2841 N

S

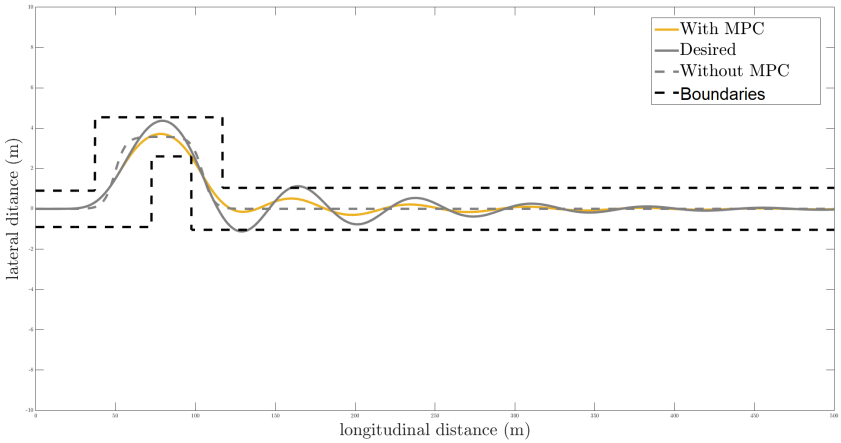

Figure 6. Vehicle trajectory from simulation of DLC at 80km/h for vehicle without ESC

5.2.2 Results for DLC at 80km/h

Simulations were performed for DLC at 80km/h, aiming to observer the ESC benefits when the vehicle speed is smaller than the constant speed assumed in the linear model used for LQR definition. Results of simulation for DLC maneuver at 80km/h are shown in Figures 7 e 6. Figure 6 shows that, without ESC assistance, the drivers perform the maneuver without losing the vehicle control, but the trajectory briefly exceeds the thresholds at the second lane changing. Whereas the trajectory of the vehicle with proposed ESC remains close to the desired path, without exceeding the boundaries of lateral displacement. From Fig. 7, one can see that the torque transferred to wheels remains null at most of the simulation time. One also can see that with this soft actuation, the proposed ESC reduces the rolling motion and the steering wheel actuation required from the driver, while remains the yaw rate close to its desired value.

5.2.3 Results for DLC at 100km/h

The second simulated scenario is the DLC maneuver at 100km/h. The purpose of this test is to observe the ESC effectiveness in a more aggressive maneuver, but with vehicle speed equal to the constant speed assumed in the linear model used in control designs, i.e with vehicle response in the trust region of LQR tuning. Figures 8 and 9 show the result obtained from this simulation.

In Fig. 9, one can observe that, without ESC assistance, the simulated driver is not able to perform this maneuver without losing the vehicle control, whereas, with the help of the proposed ESC, the maneuver is performed without the vehicle exceeding the limits of lateral displacement from the desired path.

In Fig. 9, one can observe the effectiveness of ESC activation control in avoiding unnecessary actuation, because the torque transferred to wheels remains null at most of the simulation time. And with this soft actuation, the proposed ESC is able to reduce the side-slip angle, the roll rate, the driver effort at steering wheel command and the yaw-rate error.

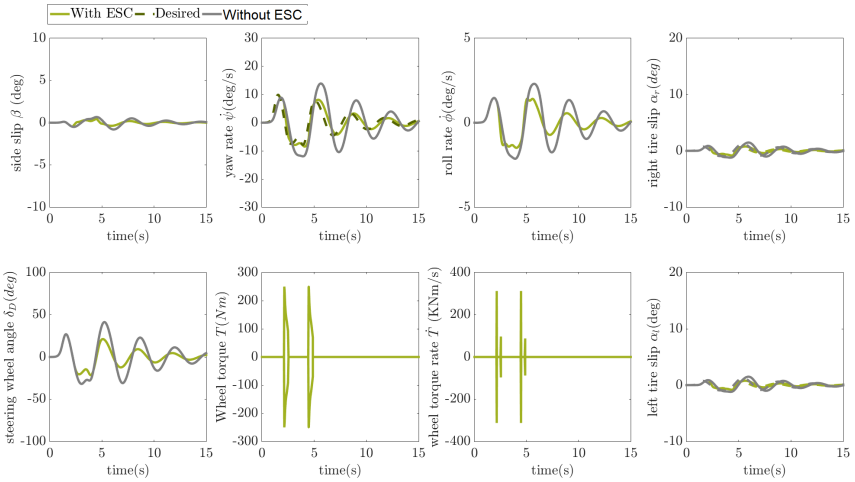

Figure 7. Results from simulation of DLC at 80km/h for vehicle without ESC

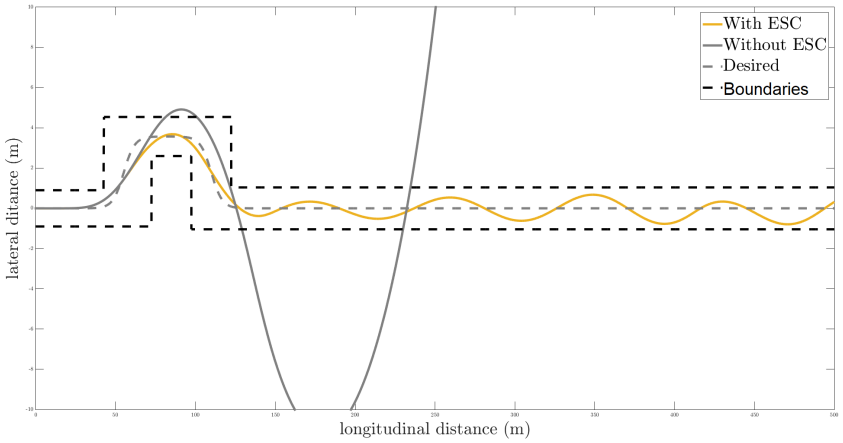

Figure 8. Vehicle trajectory from simulation of DLC at 100km/h for vehicle without ESC

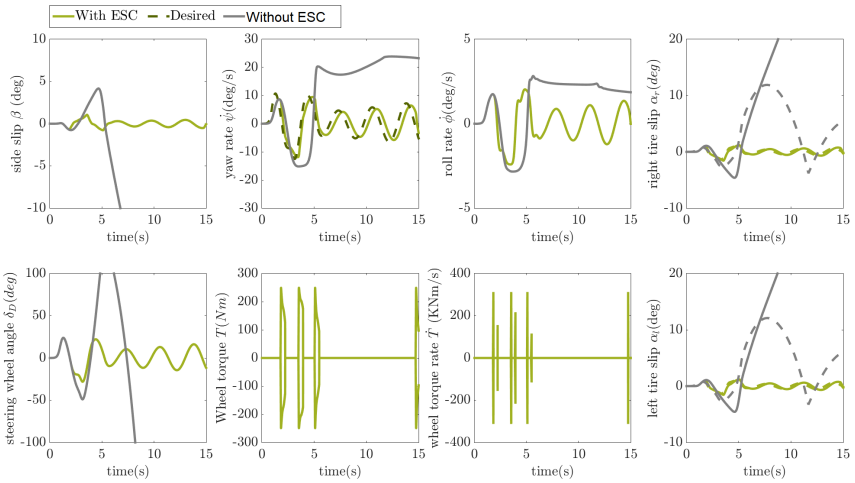

Figure 9. Results from simulation of DLC at 100km/h for vehicle without ESC

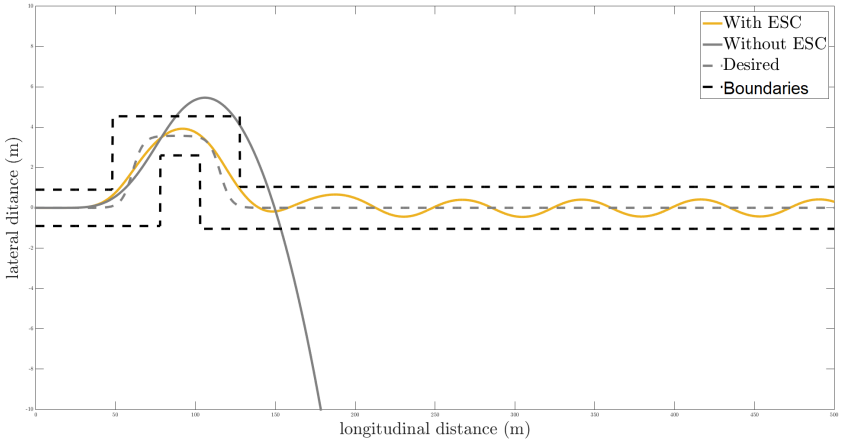

Figure 10. Vehicle trajectory from simulation of DLC at 120km/h for vehicle without ESC

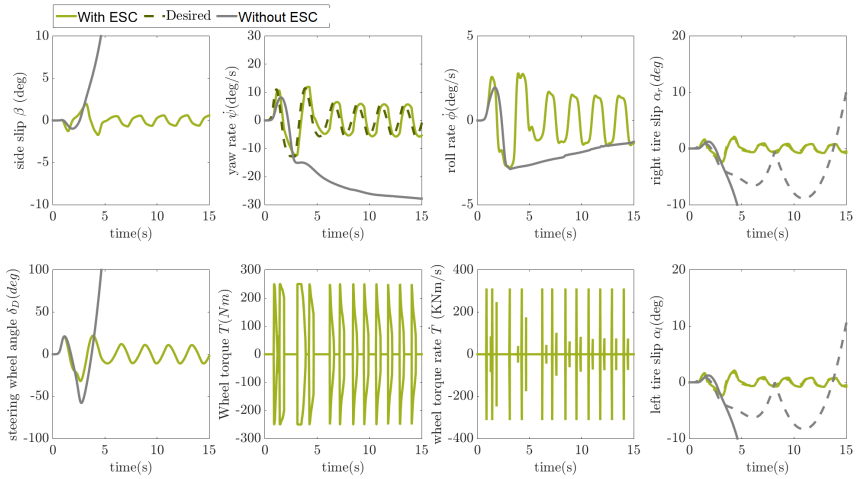

Figure 11. Results from simulation of DLC at 120km/h for vehicle without ESC

5.2.4 Results for DLC at 120km/h

The third scenario of MIL simulations is the DLC at 120 km/h. This test aims for observation of the effectiveness of the controller in a hazardous maneuver at a high speed, greater than the constant speed assumed in the linear model used for control design. Figures 10 and 11 show the results from this simulation.

From Fig. 10, one can see that, with driver ESC assistance, the drivers lose control of the vehicle, whereas with ESC assistance the maneuver is performed, over again, without crossing the boundaries of lateral displacement from the desired path.

In Fig. 11, one can see that with increasing speed, the controller needs more actuation to keep the vehicle stable, and more effort also is required from the driver. Even at 120km/h, the proposed ESC is able to reduce the side-slip angle, the roll rate, the driver effort at steering wheel command and the yaw-rate error. Another interesting result is the fact that the side-slip angles of the vehicle body and tires remain smaller than 5 degrees, this means that vehicle response remains closer to the trust region of the linear model, obtained from linearizations for small angles.

5.2.5 Results for DLC at 120km/h in presence of disturbances in model parameters

In order to observe the ESC robustness to perturbations in vehicle response in respect with the linear model used for control design, simulations also were performed to test ESC on control of a vehicle whose parameters are different from the parameters considered in the linear model. Vehicle parameters that differs from linear model is presented in Table 3, parameters not shown in Table 3 are equal to the values in Table 1.

Figures 12 and 13 show results of these simulations. By comparing results obtained for a vehicle with parameters equal and different of values assumed for control design, one can see small differences in the vehicle response, but none of them represents a loss of lateral stabilization performance. This indicates that proposed ESC has some robustness to

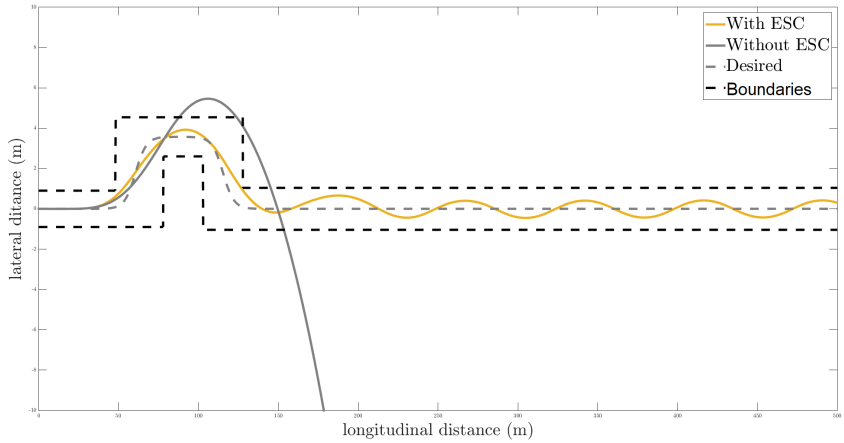

Figure 12. Vehicle trajectory from simulation of DLC at 120km/h for vehicle without ESC

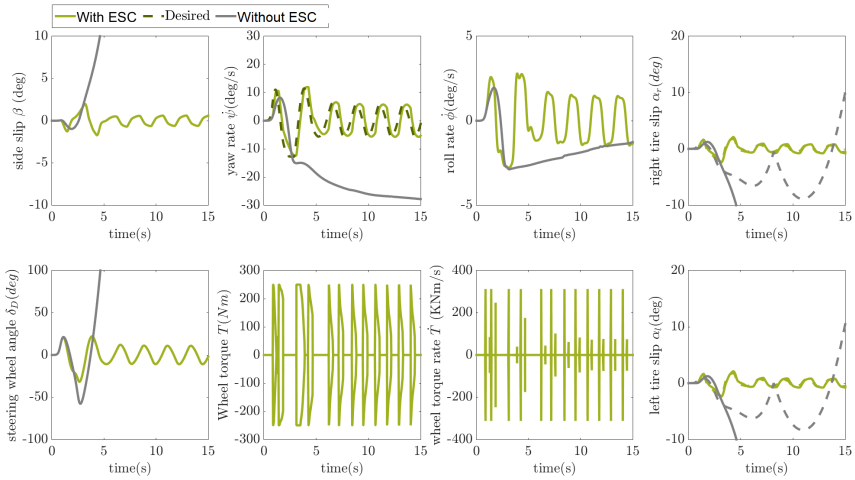

Figure 13. Results from simulation of DLC at 120km/h for vehicle without ESC

Table 3. Parameters with different values from the constants assumed in the control design. Values used in simulation of DLC at 110 km/h for vehicle simulation model and linear model with different parameters.

Param.	**Value**	**Param.**	**Value**	**Param.**	**Value**	**Param.**	**Value**
a	1.096 m	m	1177 Kg	b	1.306 m	μ	0.675

disturbances in vehicle response in respect with the predicted by the linear model used for definition of LQR gain because, in addition to differences in parameters, this scenario considers a hazardous maneuver, in which vehicle speed higher than the speed of the trim point of the control algorithm.

6. Conclusion

This paper presented the design of ESC based on discreet LQR for a continuous plant that computes the required torque transferred to wheels for correction of side-slip, yaw, and roll motions, to prevent the driver from losing control of the vehicle in dangerous corners. The control design was based on a 3DOF linear model that considers lateral, yaw and roll motions, linearized for constant longitudinal velocity equal to 100km/h, and small roll and side-slip angles. A computation simulation environment was implemented for MIL testing, combining simulations of the proposed controller, vehicle movement and driver behavior on steering command.

The DLC maneuver was simulated in the MIL environment for observation of ESC effectiveness to improve lateral stability. From the results of MIL simulations, it was observed that proposed ESC can avoid the lateral destabilization, reduce the vehicle side slipping from the desired safe trajectory. The MIL results also show that the ESC activation method contributes to avoiding unnecessary actuation, and it has the robustness to perturbation in vehicle response with respect to the predicted by the linear model used for control design.

With the increasing of vehicle speed, more actuation on traction/braking torque transferred to wheels is needed to keep the steering stable. Another effect of speed increase is the increased amplitude of the oscillation in the vehicle path after exiting the DLC maneuver, which means that ESC can keep vehicle stable, but is not able to recover the steering condition where the driver can reestablish a straight line motion. The simulated driver model does not act on vehicle acceleration to recover this steering condition. Therefore, for further investigation of the need for ESC actuation to recover the condition of easy driving, a more sophisticated driver model must be used in MIL simulations.

The next steps of this works includes the implementation of proposed ESC as electronic control unit and its evaluation with Hardware-in-the-loop simulations, the improvement of MIL environment by including a driver model that generates all the commands available for the driver in a real car, and the exploration of the benefits of advanced control techniques able to handle with constraints of actuation system, such that the proposed ESC could be applied to a vehicle without differential torque distribution system, using just a differential braking system.

7. References

Ciceo, S., Mollet, Y., Sarrazin, M., Gyselinck, J. and Auweraer, H.V.D., 2015. "Model-Based Design and Testing for Electric Vehicle Energy Consumption Analysis". *Electrotehnică Electronică Automatică*, Vol. 63, No. 4, pp. 2–5. ISSN 1582-5175.

D. Gillespie, T., 2000. "Fundamentals of vehicle dynamics". doi:10.4271/R-114.

Dahmani, H., Pagès, O. and Hajjaji, A.E., 2016. "Observer-based state feedback control for vehicle chassis stability in critical situations h." *IEEE TRANSACTIONS ON CONTROL SYSTEMS TECHNOLOGY*, Vol. 24.

Guo, H., Liu, F., Xu, F., Chen, H., Cao, D. and Ji, Y., 2017. "Nonlinear Model Predictive Lateral Stability Control of Active Chassis for Intelligent Vehicles and Its FPGA Implementation". *IEEE Transactions on Systems, Man, and Cybernetics: Systems*. ISSN 21682232.

Jalali, M., Hashemi, E., Khajepour, A., ken Chen, S. and Litkouhi, B., 2017. "Integrated model predictive control and velocity estimation of electric vehicles". *Mechatronics*. ISSN 09574158.

Jin, X.J., Yin, G. and Chen, N., 2015. "Gain-scheduled robust control for lateral stability of four-wheel-independent-drive electric vehicles via linear parameter-varying technique". *Mechatronics*. ISSN 09574158.

Jin, X.J., Yin, G., Zeng, X. and Chen, J., 2017. "Robust gain-scheduled output feedback yaw stability control for in-wheel-motor-driven electric vehicles with external yaw-moment". *Journal of the Franklin Institute*. ISSN 00160032.

Le, A.T. and Chen, C.K., 2015. "Adaptive sliding mode control for a vehicle stability system". In *2015 International Conference on Connected Vehicles and Expo (ICCVE)*. ISBN 978-1-5090-0264-1.

Li, L., Lu, Y., Wang, R. and Chen, J., 2017. "A three-dimensional dynamics control framework of vehicle lateral stability and rollover prevention via active braking with mpc". *IEEE Transactions on Industrial Electronics*. ISSN 02780046.

LIAN, Y.F., WANG, X.Y., ZHAO, Y. and TIAN, Y.T., 2015. "Direct Yaw-moment Robust Control for Electric Vehicles Based on Simplified Lateral Tire Dynamic Models and Vehicle Model". *IFAC-PapersOnLine*. ISSN 24058963.

Liu, M., Huang, J. and Chao, M., 2017. "Multi-states Combination Nonlinear Control of In-wheel-motor-drive Vehicle Dynamics Stability". In *Energy Procedia*. ISSN 18766102.

Mashadi, B., Majidi, M. and Dizaji, H.P., 2010. "Optimal vehicle dynamics controller design using a four-degrees-of-freedom model". *Proceedings of the Institution of Mechanical Engineers, Part D: Journal of Automobile Engineering*. ISSN 09544070. doi:10.1243/09544070JAUTO1280.

Mashadi, B., Mostaani, S. and Majidi, M., 2011. "Vehicle stability enhancement by using an active differential". In *Proceedings of the Institution of Mechanical Engineers. Part I: Journal of Systems and Control Engineering*. ISSN

09596518.

Mousavinejad, I., Zhu, Y. and Vlacic, L., 2015. "Control Strategies for Improving Ground Vehicle Stability State-of-the-art Review". In *2015 10th Asian Control Conference (ASCC)*.

Nahidi, A., Kasaiezadeh, A., Khosravani, S., Khajepour, A., Chen, S.K. and Litkouhi, B., 2017. "Modular integrated longitudinal and lateral vehicle stability control for electric vehicles". *Mechatronics*. ISSN 09574158.

Pacejka, H.B., 2006. *Tyre and Vehicle Dynamics (Second Edition)*. Butterworth-Heinemann, Oxford, second edition edition. ISBN 978-0-7506-6918-4.

Plummer, A.R., 2006. "Model-in-the-loop testing". *Proceedings of the Institution of Mechanical Engineers. Part I: Journal of Systems and Control Engineering*, Vol. 220, No. 3, pp. 183–199. ISSN 09596518. doi: 10.1243/09596518JSCE207.

Rajamani, R. and Piyabongkarn, D.N., 2013. "New paradigms for the integration of yaw stability and rollover prevention functions in vehicle stability control". *IEEE Transactions on Intelligent Transportation Systems*. ISSN 15249050.

Reński, A., 2001. "Identification of driver model parameters". *International Journal of Occupational Safety and Ergonomics*, Vol. 7, No. 1, pp. 79–92. ISSN 10803548. doi:10.1080/10803548.2001.11076478.

Shoutao Li, Di Zhao, Luyu Zhang, Y.T. and College, 2017. "Lateral stability control system based on cooperative torque distribution for a four in-wheel motor drive electric vehicle". In *Proceedings of the 36th Chinese Control Conference*. Dalian, China, Vol. 105, pp. 2825–2830. ISSN 18766102.

Yogurtcu, I., Solmaz, S. and Baslamish, S.C., 2015. "Lateral stability control based on active motor torque control for electric and hybrid vehicles". In *2015 IEEE European Modelling Symposium (EMS)*. pp. 213–218. ISBN 978-1-5090-0206-1.

Zheng, S., Tang, H., Han, Z. and Zhang, Y., 2006. "Controller design for vehicle stability enhancement". *Control Engineering Practice*, Vol. 14, pp. 1413–1421. ISSN 09670661.

Zheng, Y. and Shyrokau, B., 2019. "A Real-Time Nonlinear MPC for Extreme Lateral Stabilization of Passenger Vehicles". *Proceedings - 2019 IEEE International Conference on Mechatronics, ICM 2019*, Vol. 1, pp. 519–524. doi: 10.1109/ICMECH.2019.8722930.

Zhou, H. and Liu, Z., 2010. "Vehicle yaw stability-control system design based on sliding mode and backstepping control approach". *IEEE Transactions on Vehicular Technology*, Vol. 59, pp. 3674–3678. ISSN 00189545.

8. RESPONSIBILITY NOTICE

The following text, properly adapted to the number of authors, must be included in the last section of the paper: The author(s) is (are) the only responsible for the printed material included in this paper.